A scalable concept for micropower generation using flow-induced self-excited oscillations

D. St. Clair, A. Bibo, V. R. Sennakesavababu, M. F. Daqaq, and G. Li[a)]
College of Engineering and Science, Clemson University, South Carolina 29634, USA

(Received 24 January 2010; accepted 18 March 2010; published online 8 April 2010)

Inspired by music-playing harmonicas that create tones via oscillations of reeds when subjected to air blow, this paper entails a concept for microwind power generation using flow-induced self-excited oscillations of a piezoelectric beam embedded within a cavity. Specifically, when the volumetric flow rate of air past the beam exceeds a certain threshold, the energy pumped into the structure via nonlinear pressure forces offsets the system's intrinsic damping setting the beam into self-sustained *limit-cycle* oscillations. The vibratory energy is then converted into electricity through principles of piezoelectricity. Experimental and theoretical results are presented demonstrating the feasibility of the proposed concept. © *2010 American Institute of Physics*. [doi:10.1063/1.3385780]

Technological advances in electronics and microfabrication techniques led to the development of very compact low-power consumption devices that require minute amount of power to function.[1,2] Currently, these devices are being powered and maintained by batteries that have not kept pace with such devices demands especially in terms of energy density.[3] In addition, batteries require regular replacement and recharging which can be a cumbersome and expensive task especially for systems installed in remote locations.

To overcome these issues, current research trends call for harnessing energy from the environment to power and maintain these low-power consumption devices. Toward that end, many electromechanical systems have been proposed to convert ambient energy such as wind and vibration into electricity. For instance, many variations in the traditional rotary-type generators have been implemented for wind energy harvesting. However, such wind turbines suffer from critical scalability issues because their performance drops significantly with their size.[4] In addition, fabrication of small-scale rotary-type generators that require magnets, windings, and blades can be very complex and expensive making their actual implementation for small-scale applications a formidable task.

Other concepts based on vibration energy harvesting have also evolved to transform mechanical motions directly into electricity by exploiting the ability of active materials to generate an electric potential in response to mechanical stimuli and external vibrations.[2,5] However, this technology also suffers from several drawbacks. First, a vibrations source is not always available where electronic devices are designed to operate. Second, such devices have a critical shortcoming in their operation concept. These harvesters operate efficiently only within a narrow frequency bandwidth where the excitation frequency is very close to the fundamental frequency of the harvester (resonance condition). Small variations in the excitation frequency around the harvester's fundamental frequency drops its small energy output even further making the energy harvesting process inefficient.[2,6–8]

Motivated by this need for portable yet scalable high-power density and low-maintenance energy harvesters, we propose a concept for a micropower generator that uses self-excited limit-cycle oscillations of a piezoelectric beam to harness wind energy and maintain low-power consumption devices. Inspired by music playing harmonica, the harvester shown in Fig. 1 consists of a piezoelectric cantilever unimorph structure embedded within a cavity to mimic the vibration of the reeds in a harmonica when subjected to air blow. The operation principle of the harvester is simple. Wind blows into the chamber and the air pressure in the chamber increases. The increased air pressure bends the beam and opens an air path between the chamber and the environment. As the air passes through the aperture, the pressure in the chamber decreases. The mechanical restoring force pulls the beam back decreasing the aperture area and the process is repeated. These periodic fluctuations in the pressure cause the beam to undergo *self-sustained* oscillations. The resulting periodic strain in the piezoelectric layer produces an electric field which can be channeled as a current to an electric device.

The significance of this concept for micropower generation stems from its ability to eliminate the shortcomings of traditional vibration-based energy harvesters and small size wind turbines while, at the same time, combining aerodynamics with vibrations to generate the necessary power. On one hand, this concept is based on transforming vibrations to electricity but does not require an external vibration source eliminating the bandwidth issues associated with resonant

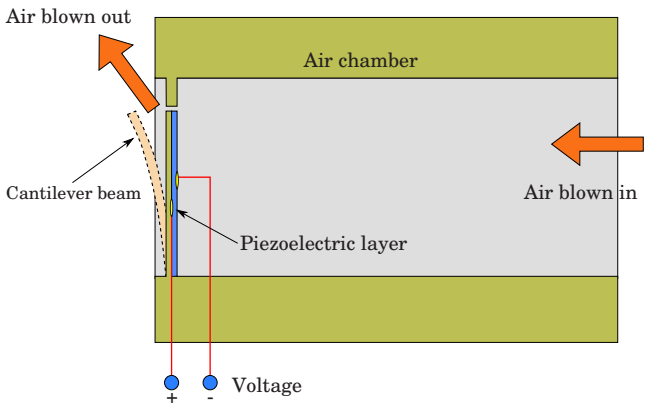

FIG. 1. (Color online) Wind energy harvest system.

[a)]Electronic mail: gli@clemson.edu.

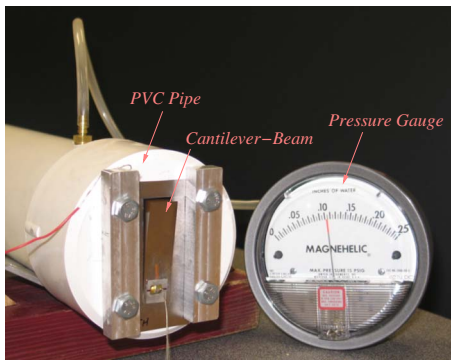

FIG. 2. (Color online) Wind-driven autonomous beam vibrations.

vibratory energy harvesters. On the other hand, while this device depends on the presence of an aerodynamic energy field, it does not suffer from the scalability issues that hinder the efficiency of small size wind turbines.

From a mathematical point of view the resulting self-excited oscillations of the beam is a nonlinear phenomenon that mimics the dynamics of the widely celebrated Van der Pol oscillator whose equation of motion is given by

$$\ddot{x} + \mu(x^2 - 1)\dot{x} + x = 0 \quad \mu \geq 0. \tag{1}$$

The Van der Pol oscillator is a simple harmonic oscillator but with a nonlinear damping term $\mu(x^2-1)\dot{x}$. For small oscillations, $|x|<1$, the damping is negative pumping energy into the structure and causing small-amplitude oscillations to grow. However, when $|x|>1$, the damping becomes positive causing large amplitudes to decay. At one point, the energy dissipated over one cycle balances the energy pumped and the system settles into limit-cycle oscillations. In a similar manner, self-excited oscillations of the beam occur when the volumetric flow rate of air past the cantilever is large enough such that the energy pumped into the structure via nonlinear pressure forces offsets the intrinsic damping in the system which consists of structural damping and electric damping due to energy generation. One can also think of this process as a nonlinear feedback mechanism in which the motion of the cantilever produces a disturbance in the potential flow that feeds enough energy back to the structure to overcome the internal damping. The excitation responsible for this nonlinear feedback is thought of as a combination of the pressure induced by variations in the velocity due to the complex evolution of the aperture area, the inertial effect of the unsteady flow past the cantilever, and the acoustic pressure waves that develop within the chamber.[9–11]

The onset of the limit-cycle oscillations is governed by a threshold combination of the flow and design parameters known as the *Hopf bifurcation* point. Below that threshold, the energy pumping mechanism cannot overcome the damping mechanism and the structure settles at an equilibrium. Beyond that threshold, the nonlinear pressure forces overcome the intrinsic damping and the beam starts to oscillate. When the Hopf bifurcation is *supercritical*, stable small-amplitude limit-cycle oscillations about the former static position are born. On the other hand, when the Hopf bifurcation is *subcritical*, the response jumps to a distant attractor.

To determine the cut-in wind speed of the generator (Hopf bifurcation point), a simple lumped-parameters model is formulated.[12,13] A single-mode equation representing the

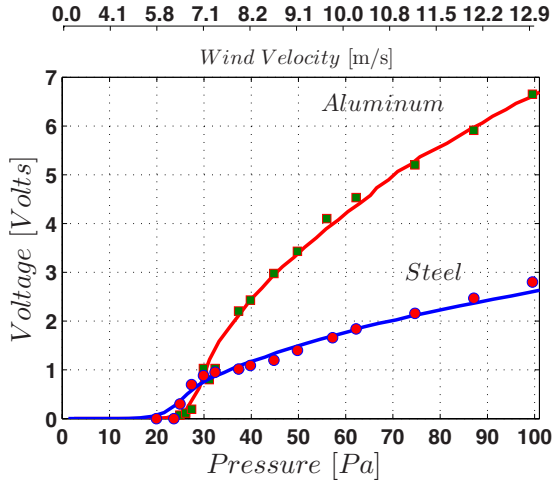

FIG. 3. (Color online) Output voltage as a function of the air pressure (dots: experimental results, curves: simulation results).

temporal evolution of the beam's tip deflection, x, can be written as

$$\frac{d^2x}{dt^2} + 2\zeta\omega_0\frac{dx}{dt} + \omega_0^2 x + \beta x^3 = \frac{1.5p(t)}{\rho h} + \frac{\alpha V_e}{bL\rho h}, \tag{2}$$

where t denotes time, ζ is the mechanical damping ratio, $p(t)$ is the air pressure exerted on the top surface of the beam measured relative to the ambient pressure, α is an electromechanical coupling term, β is a cubic nonlinearity coefficient used to account for geometric nonlinearities in the beam response, and V_e is the voltage developed across the piezoelectric layer. The natural frequency, ω_0, of the multilayer beam can be approximated as $\omega_0=\sqrt{K_{\text{eff}}/m_{\text{eff}}}$, where K_{eff} and m_{eff} are the effective stiffness and effective mass of the beam, respectively. Assuming the piezoelectric layer is mechanically negligible compared to the cantilever beam due to its small size and thickness, the effective stiffness of the beam can be approximated as $K_{\text{eff}}=bEh^3/4L^3$, where b, L, h, and E are the width, length, height, and Young's modulus of the beam, respectively. The effective mass of the beam can be approximated as $m_{\text{eff}}=0.24bL\rho h$, where ρ is the mass density of the beam material.

Using Kirchhoff's law, the induced voltage can be further related to the piezoelectric capacitance and electric load according to[13]

$$C_p\frac{dV_e}{dt} + \frac{V_e}{R} + \alpha\frac{dx}{dt} = 0, \tag{3}$$

where R is the electric load and C_p is the piezoelectric capacitance. Using the steady Euler–Bernoulli equation, $p(t)$ can be related to the volumetric air flow rate through the aperture, $U(t)$, as

$$p = \frac{\rho_a U(t)^2}{2C^2F(x)^2}, \tag{4}$$

where ρ_a is the air density, $C=0.61$ is the flow contraction coefficient for flow through a sharp edged slit, $F(x)=(b+0.8L)x$ is the total exit area of the aperture, and $U(t)$ is the volume flow through the beam opening. Finally, using the continuity equation, we can relate $p(t)$ to the volumetric flow rate and the tip deflection via

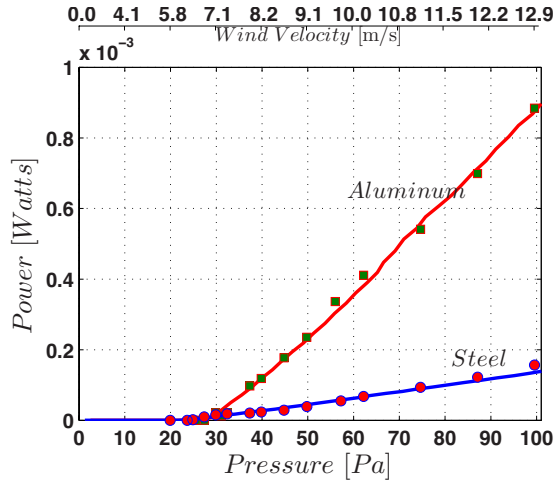

FIG. 4. (Color online) Peak output power as a function of the air pressure (dots: experimental results, curves: simulation results).

$$\frac{dp}{dt} = \frac{\rho_a c^2}{V}\left(U_0 - U - 0.4bL\frac{dx}{dt}\right), \tag{5}$$

where c is the speed of sound, V is the volume of the chamber and U_0 is the input volumetric flow rate. By solving Eqs. (2)–(5), the response characteristics of the system can be determined. The output power can be obtained via $P=|V_e|^2/R$.

Figure 2 depicts the experimental configuration employed to investigate the feasibility of the proposed concept. A 2.4 l air chamber is constructed using a polyvinyl chloride (PVC) pipe with inside diameter of 76.2 mm, closed with two PVC caps. On one end cap, the cantilever beam is mounted over the aperture/slot as shown in the figure. To accommodate the beam, the aperture is made slightly larger than the beam providing a gap of about 0.3 mm. From the other end of the chamber, air is supplied using an air pump through a small hole at the center of the cap. To compare the performance of different configurations, beams are cut from a 0.3 mm thick aluminum sheet and a 0.15 mm thick steel sheet. The length and width of the beams are 58 mm and 16 mm, respectively. For power generation, a PSI-5A4E PZT thin plate was bonded onto the outer surface of the beam. The dimensions of the PZT plate is 12 mm in width, 13 mm in length, and 0.127 mm in thickness.

In the experiments, the air pressure is increased incrementally from 0 to 100 Pa. At each step, the mean pressure at the beam surface is measured using a pressure gauge and the corresponding output voltage at different pressures is recorded. The air pressure is then slowly decreased from 100 Pa until the beam vibration ceases. Once again, the output voltage at different pressures is recorded. It was observed that there are not much differences between the voltage values measured at both directions of the pressure sweep. As such, only the average value is reported. Figures 3 and 4 depict variation in the voltage and output power of the device with the chamber air pressure and the corresponding wind speed over an electric load of 49.65 kOhm. The experimental results are also compared to numerical simulations obtained via long-time integration of Eqs. (2)–(5). Numerical parameters corresponding to the experimental setup are listed in Table I. As shown in the figures, the steel and aluminum beams are activated at threshold pressures of 25 Pa and 29 Pa, respectively. This corresponds to moderate cut-in wind speeds of approximately 6.45–6.95 m/s. The 7% drop in the cut-in wind speed associated with the steel beam can be mainly attributed to the reduced thickness (stiffness) of the beam when compared to the Aluminum beam. However, while the cut-in wind speed using the steel beam is slightly smaller, the measured output voltage and power using the Aluminum beam are much higher. This is believed to be mainly due to the larger thickness of the Aluminum beam which yields larger mechanical strain in the piezoelectric sheet. This, in turn, produces a larger output voltage.

TABLE I. Numerical values of the parameters used in the simulations.

Beam	ζ	ω_0 (rad/s)	C_p (nF)	α (N/V)	β [1/(ms)]
Aluminum	0.03	527	19.6	0.000259	4.5×10^{14}
Steel	0.04	257	19.6	0.000187	7×10^{14}

The experiments further reveal that the transition from the static position to the limit-cycle oscillations is continuous. This indicates that the bifurcation is *supercritical* for the chosen design parameters which agrees with the predictions of the mathematical model. The 0.1–0.8 mW of output power attained using the Aluminum beam at wind speeds ranging between 7.5 and 12.5 m/s clearly demonstrate the potential for using such concept to power and operate many microdevices.[14] However, such results by no means represent the optimal performance of this device. For instance, although the current prototype provides a maximum power density (around 0.02 mW/cm^2) similar to that of a previously reported windmill-type piezoelectric wind energy harvester[15] along with the advantage of less structural and design complexities (e.g., blades and bearings), its cut-in wind speed is higher. As the theoretical model and the experiments clearly demonstrate the interconnected dependence of the output power on the design parameters of the harvester, it is believed that the output power as well as the cut-in wind speed of the device can be significantly enhanced using an optimization analysis of the theoretical model.

[1] S. Roundy, P. K. Wright, and J. Rabaey, Comput. Commun. **26**, 1131 (2003).
[2] S. Roundy, J. Intell. Mater. Syst. Struct. **16**, 809 (2005).
[3] J. A. Paradiso and T. Starner, IEEE Pervasive Comput. **4**, 18 (2005).
[4] P. Mitcheson, E. Yeatman, K. Rao, S. Holmes, and T. Green, Proc. IEEE **96**, 1457 (2008).
[5] H. Sodano, G. Park, and D. J. Inman, Strain **40**, 49 (2004).
[6] N. duToit and B. Wardle, AIAA J. **45**, 1126 (2007).
[7] A. Erturk and D. Inman, J. Vib. Acoust. **130**, 041002 (2008).
[8] J. Renno, M. F. Daqaq, and D. J. Inman, J. Sound Vib. **320**, 386 (2009).
[9] A. O. St. Hilaire, J. Sound Vib. **47**, 185 (1976).
[10] N. H. Fletcher, J. Acoust. Soc. Am. **93**, 2172 (1993).
[11] A. Z. Tarnopolsky, J. Lai, and N. Fletcher, J. Sound Vib. **247**, 213 (2001).
[12] A. Z. Tarnopolsky, N. H. Fletcher, and J. C. S. Lai, J. Acoust. Soc. Am. **108**, 400 (2000).
[13] T. Osorio and M. F. Daqaq, J. Intell. Mater. Syst. Struct. **20**, 2003 (2009).
[14] W. Bracke, P. Merken, R. Puers, and C. Van Hoof, Sens. Actuators, A **135**, 881 (2007).
[15] S. Priya, Appl. Phys. Lett. **87**, 184101 (2005).